



Brain Glial Cell Tumor Classification through Ensemble Deep Learning with APCGAN Augmentation

T. Deepa^{1*}, Ch. D. V. Subba Rao²

¹Department of Computer Science and Engineering, Sri Venkateswara University College of Engineering, Andhra Pradesh, India

* Corresponding Author Email: deepa.thota0607@gmail.com ORCID: 0009-0006-0802-8050

²Department of Computer Science and Engineering, Sri Venkateswara University College of Engineering, Andhra Pradesh, India

Email: subbarao_chdv@hotmail.com ORCID: 0000-0001-0302-2010

Article Info:

DOI: 10.22399/ijcesen.803
Received : 23 September 2024
Accepted : 31 December 2024

Keywords:

Brain Tumor,
Classification,
Data Augmentation,
Generative Adversarial Networks,
Ensemble Learning

Abstract:

Classification of brain tumor plays a vital role in medical imaging for accurate diagnosis, treatment, and monitoring. Deep learning approaches have gained significant traction in this industry because of their ability to extract relevant features from medical images. The research suggests employing an ensemble classifier with a weighted voting mechanism to categorize glial cell brain malignancies such as Astrocytoma, Glioblastoma multiforme, Oligodendroglioma, and Ependymoma. The proposed ensemble technique employs three main classifiers: Convolutional Neural Network (CNN), Deep Convolutional Long Short Term Memory (C-LSTM), and Deep Convolutional Neural Network + Conditional Random Fields (DCNN+CRF). Deep learning algorithms require a huge amount of input data to avoid overfitting. The Adaptive Progressive Convolutional Generative Adversarial Networks (APCGANs) are used to produce realistic artificial images to efficiently train the proposed methodology. Overall, the proposed ensemble method with weighted voting strategy consistently outperforms the other tested algorithms (CNN, C-LSTM, and DCNN+CRF). Ensemble method attained an accuracy of 99.4 %, recall - 99.1%, precision- 98.0%, and F1-score of 99.2%. Ensemble method consistently demonstrates superior performance in accurately classifying brain tumors, making it a promising algorithm for brain tumor analysis tasks.

1. Introduction

In 2020, World Health Organization (WHO) indicators demonstrate that there are 308,102 individuals identified with brain tumors. Among all central nervous system tumors Brain tumors account for 85% to 90%. Brain tumors are graded 10th leading sources of death in adults and kids. In 2020 it is assessed that 251,329 people were deceased with primary brain tumors worldwide [1]. Brain tumors are the utmost perplexing and multifaceted medical conditions to treat. Generally, they fall into two categories: primary and metastatic. Primary tumors originate within the brain, while metastatic tumors, in contrast, develop when cancer cells migrate from various parts of the body to the brain. The glial cells in the central nervous system, also known as neuroglia, provide support and protection to nerve cells. The cells are in different shapes, sizes, and

categories, each with its own function. Glia is responsible for both the structural and physiological support of the nervous system. The neuroglia wipes deceased neurons, synchronize nerve impulses and normalize brain metabolism [2]. The tumors in the brain glial cells are termed as gliomas. Gliomas are the utmost common and death causing primary tumors. Gliomas are categorized in to diverse classes based on the glial cell it instigates from and their individualities [3]

Astrocytoma, Glioblastoma multiforme, Medulloblastoma, Oligodendroglioma and Ependymoma are the categories of glial cell tumors. Astrocytoma belongs to a collection of brain tumors that instigate from star shaped cells called astrocytes. The grading of Astrocytomas depends on factors, like location, size and how far the tumor cells have spread. Grade I and II Astrocytomas grow slowly. Usually stay confined to areas of the brain. In

contrast Grade III and IV Astrocytomas are highly destructive. Spread rapidly causing neurological symptoms [4]. Glioblastoma multiforme (GBM) is the most common type of brain tumor, accounting for approximately half of all cases. It is characterized by tumor growth, patterns of growth and a high mortality rate. GBM tumors typically develop within the hemispheres of the brain. They are particularly challenging to treat due to their invasive nature. Medulloblastoma is the menacing brain tumor in children representing nearly 20% of all infantile brain tumors. It originates in the cerebellum. Often presents with symptoms such as headaches, vomiting and difficulties with coordination. Additionally it can lead to hydrocephalus—a condition characterized by an accumulation of fluid, in the brain. The type of brain tumor that develops from oligodendrocytes is called an oligodendroglioma. These cells play an important role in creating the myelin sheath that covers nerve fibers. This particular tumor tends to grow and commonly affects the temporal lobes of the brain. Symptoms typically include seizures, headaches and various neurological problems [5]. Ependymomas are rare brain tumors that descend from ependymal cells lining the ventricles and spinal cord. They can manifest at any age and may exhibit a broad spectrum of neurological symptoms, contingent upon their location within the brain or spinal cord. For the purpose of diagnosis, prognosis, and treatment planning, it is essential to exactly categorize these brain tumors. While MRI and CT scans serve as ordinary instruments for visualizing brain tumors and evaluating their size, location, and morphology, advanced imaging modalities like diffusion tensor imaging (DTI) and perfusion imaging proffer additional glimpses into tumor growth and blood flow patterns. Machine learning techniques, predominantly convolutional neural networks (CNNs), have the capability in automatically categorizing brain cancers based on MRI data. Tough tumor classification is achieved by these techniques, which make advantage of MRI scan properties such texture, shape, and intensity [6]. By finding pertinent features in MRI scans, deep learning—and CNNs in particular—has been helpful in improving the classification accuracy of brain cancers. Ensemble learning methods, combines predictions from multiple models, have also proven effective in enhancing the precision of brain tumor classification. Using Transfer learning, the pre-trained models are adapted for new tasks, further refines brain tumor categorization [7]. Recognizing brain tumors accurately is critical for effective treatment planning and eventually improving patient outcomes. Advanced imaging technologies, coupled with machine learning, deep learning, and ensemble

learning, show promising ways to improve the accuracy of brain tumor classification.

Ongoing research is required to develop even more accurate and robust categorization algorithms that can help doctors make well-informed decisions about patient treatment. Brain tumor forms such as Astrocytoma, Glioblastoma multiforme, Oligodendroglioma, and Ependymoma require a mix of imaging techniques, histological examination, and genetic study. These techniques provide useful information for diagnosing and determining the precise tumor type and grade, which aids in treatment decisions and prognosis evaluation. The proposed effort intends to build on existing research and approaches to improve the accuracy and heftiness of categorization models. Even with the multiple proposed strategies, distinguishing between different tumor classifications remains a significant difficulty. Furthermore, more efficient and scalable approaches for dealing with larger datasets are required.

Based on the existing literature, multiple researchers have attempted brain tumor classification, outlining various groups such as glioma, meningioma, and pituitary tumors. [8-11] Others have pursued binary classification, distinguishing benign from malignant tumors [12-15]. Notably, some tumors originate in glial cells, including Astrocytoma, Glioblastoma multiforme, Medulloblastoma, Oligodendroglioma, and Ependymomas, and these can be particularly perilous, often resulting in fatality. Medulloblastoma is particularly prevalent in children. Our research is specifically centered on the classification of adult glial cell tumors.

The primary objective of this ensemble model, featuring APCGANs, is to provide a methodology that facilitates the multiclass classification of glial cell tumors by analysing MRI sequences. The key components of our anticipated model are as follows:

1. We propose an efficient method for classifying glial cell tumors into subtypes, including Astrocytoma, Glioblastoma multiforme, Oligodendroglioma, and Ependymomas.
2. Pre-processing is undertaken to standardize intensities, and a registration algorithm is employed to align voxel size and orientation.
3. Our method leverages multimodal data, specifically a 4D tensor encompassing all four MRI modalities for a single patient.
4. To address the issue of limited data, we employ Adaptive Progressive Convolutional Generative Adversarial Networks (APCGAN) to generate realistic synthetic images.
5. We employ an ensemble approach, combining CNN, C-LSTM, and DCNN+CRF with a weighted voting method to perform classification.

Overall, our proposed ensemble model with APCGANs for glial cell brain tumor classification is to advance the accuracy, robustness, efficiency, and scalability of the classification models to enable more accurate diagnosis and treatment planning for patients.

2. Related Works and Motivation

Currently, deep learning techniques are being explored to cultivate more exact and well-organized methods for classifying brain tumors. For example, researchers are using convolutional neural networks (CNNs) which examine MRI scans and differentiates tumors with high accuracy. In terms of research, plentiful studies have been performed to develop and refine the classification of these brain tumors. For example, a 2016 study published in *Neuro-Oncology* used a combination of molecular and imaging data to develop a new classification system for gliomas. Another study published in *Scientific Reports* in 2020 used deep learning techniques to classify gliomas based on MRI imaging data. Overall, the classification of Astrocytoma, Glioblastoma multiforme, Medulloblastoma, Oligodendroglioma, and Ependymomas has evolved significantly over the years. With continued research and technological advancements, it is likely that more accurate and efficient methods for classification will be developed in the future.

Currently, many researchers are using an ensemble learning strategy because it gives better results compared to the methods we use now. Zahoor et al. [8] introduced the DHL-DC framework for the analysis of MR images to detect tumors. The framework contains two phases. As a first step, ensemble classifiers with deep-boosted features space (DBFS-EC) are offered in identifying tumors. As a second step hybrid features fusion grounded brain tumor detection (HFF-BTC) is implemented in the direction of categorizing tumors into different classes. Authors fused static and dynamic features to create a feature space. The dynamic features are excavated with CNN and the static attributes are mined with a histogram of gradient feature descriptors. The author's mentioned that the framework outclassed the state-of-the-art procedures by an accurateness of 99.20%.

In reference [9], a study unraveled a groundbreaking hybrid methodology for categorizing tumors within 3D MR images. Initially, the input images undergo a transformative normalization process using a min-max normalization approach, followed by a dynamic resizing technique to amplify performance. The ingenious researchers crafted a fusion model that melds a 3D CNN with Long Short Term Memory

(LSTM) networks, where every layer enveloped by a time-distributed function. Significantly, all MRI sequences are amalgamated into a singular input dataset, defying convention. To evaluate the awe-inspiring efficacy of this process, they harnessed K-fold cross-validation, delving into an array of K values, and the outcome was nothing short of astonishing—an accuracy of a mind-boggling 98.90%. In reference [10], another study divulged an enthralling exploration, where the ingenious researchers harnessed the power of a available Inceptionv3 model to extract useful attributes from the data, thereby unfurling a score vector of extraordinary proportions. This score vector, a veritable treasure trove of information, was then thrust into the depths of a quantum variational network, where it unfurled its enigmatic prowess in classifying tumors into multiple categories. In addition to this enthralling feat, the authors deployed a formidable model known as SegNetwork, a master of its craft, capable of delineating and isolating the healthy tissues from the tumor region. Authors in [11] implemented preprocessing and post processing with MRA-UNet to achieve higher accurateness.

Authors in [12] employed a transfer learning strategy for tumor detection. Preprocessing was utilized as the initial step, including data augmentation for the input data. Multiple available models were employed to excerpt features, and these traits were then passed to various classifiers. The accuracy of feature extractor and classifier was evaluated by means of 10-fold cross-validation, and concluded that VGG19-SVM yielded highest performance. In [13], a hybrid deep learning model combining CNN and LSTM was proposed. Preprocessing involved normalization, resizing, extreme points are calculated to crop images and noise removal through erosion and dilation. The features are extracted with CNN and a hybrid CNN-LSTM method was employed for binary classification. This hybrid model reached an accuracy of 99.1%.

Murthy et al. [14] proposed an ensemble classification methodology for tumor classification. The methodology includes preprocessing of the images through the application of a median filter to eradicate blare and histogram equalization for contrast improvement. Authors introduce a Segmentation using an Adaptive Fuzzy Deformable Fusion (AFDF) approach that associates snake deformable approach in addition to Fuzzy C-Means Clustering (FCM). For the purposes of classification, authors implemented Ensemble Classification with Optimized Convolutional Neural Network with (OCNN-EC). In a similar vein, Kriti Raj et al. [15] propose an ensemble scheme for multi-class categorization of tumors, specifically Meningioma, Astrocytoma, Oligodendroglioma and Glioblastoma

multiforme. The authors employ fusion of feature mining approaches, Discrete Wavelet Transform (DWT) with Gradient Grey Level Co-occurrence Matrix (GLCM), and other based on Grey Level Run Length Matrix (GLRLM), DWT and Local Binary Pattern (LBP).

Furthermore, S.A. Nawaz et al. [16] develop a framework for the classification of tumors in to multiple classes. Authors enhance MR images using a Kernel-Sobel-Low Pass (K-S-L) filter. To generate Region of interest (ROI) segmentation is accomplished through Threshold and clustering-based methods. Gradient features and Texture features are mined from the ROI to create a feature vector. Choose the most significant attributes from the feature-vector employing the correlation-based feature selection (CFS) procedure. These features are fed to multiple classifiers (MLP, J48, MB, and RT) through 10-fold cross-validation to access the performance. S. Asif et al. [17] presented a Transfer learning methodology in which four pre-trained models are utilized to excerpt features along with weights from a large dataset and these learning's are used to categorize tumors from a small dataset. They used multiple optimizers and 3 dense layers with a soft-max classifier. The authors implemented data augmentation and hyper parameter tuning to attain extraordinary performance.

Suchismita Das et al. [18] introduced a two-step ensemble deep architecture for tumor subdivision. In the first step, all the MRI modalities (FLAIR, T1, T1ce, and T2) are passed as input to the three diverse schematic segmentation algorithms (Encoder-Decoder, SegNet, and UNet) for generating feature maps. The feature maps were fused to produce a single maximized feature map to carry out segmentation. The model has been validated on TICA 2017 dataset. Kang, J et al. [19] designed a completely programmed fusion approach for brain tumor grouping. The classification is performed in three phases. 1. Deep features are extracted employing pre-trained models. 2. Topmost three features are carefully chosen using machine learning models. 3. Created an ensemble model to achieve perfect classification. The model is assessed on two public datasets. Garge et al. [20] wished for a binary classification of tumors into benign or malignant. To reach this, the authors used a hybrid ensemble approach by combing 3 base learners (KNN, RF, and DT) with the majority voting method. Images are segmented with Otsu's thresholding process and thirteen features are mined using PCA and SWT (stationary wavelet transforms).

P. Ramya et al. [21] implemented an ensemble learning method to accomplish segmentation and for further classification. The process utilized laplacian cellular automata filter to eradicate the Gaussian

noise, the instrumental noise that may be added during scanning. To perform segmentation authors formed an ensemble of three clustering algorithms (K-means, Gaussian mixture model clustering, and Fuzzy based clustering) using the consensus ensemble function. A deep super classifier is proposed to organize the images into multiple classes. The proposal is tested on TICA 2015 dataset. In their study, Rezae et al. [22] projected an ensemble classifier with weighted voting method. The authors employed median and Wiener filters for the purposes of de-noising and image enhancement. In order to segment tumors from healthy tissues, a linear kernel function along with support vector machine (SVM) was involved. Statistical features are mined by means of Dominant Gray Level Run Length Matrix (DRLM), Gray Level Co-occurrence Matrix (GLCM), and Bag of Words (BoW) approach. Differential Evolution framework was applied to determine essential features from the feature vector. An ensemble classifier was constructed using three base learners, namely weighted kernel SVM, histogram intersection kernel SVM and K-nearest neighbors (KNN). Classification was performed using the weighted voting method. Several authors have implemented innumerable ways and means to address brain tumor classification.

3. Proposed Method

Over the last decade, numerous researchers have increasingly embraced deep learning techniques to address challenges in image classification. Among these methods, Convolutional Neural Networks (CNN) stand out as the most successful and efficient approach in the field of computer vision. CNN finds application in diverse areas such as pattern recognition, object detection, picture segmentation, and image classification. The remarkable achievements of CNN have prompted many researchers to conduct their studies using this methodology, resulting in a surge of simulations in recent literature [23]. In this work, we propose a novel approach that leverages an ensemble of three distinct classifiers: CNN, C-LSTM, and DCNN with CRF, employing a weighted voting strategy for optimal results. Figure 1 illustrates the architecture of the proposed method. The ensemble method is aimed to combine the results of three classifiers using a weighted voting mechanism, ensuring accuracy and precision in the final outcomes.

The workflow starts with a pre-processing step, which consist of intensity normalization and the merging of all four modalities (T1, T2, T1CE, and FLAIR). This merging results in multimodal data, effectively increasing the available data for training.

To further improve the dataset for training, we employ the Adaptive Progressive Convolutional Generative Adversarial Network (APCGAN) to generate synthetic images. This augmentation process enhances the robustness and effectiveness of the proposed method, improving its performance in image classification tasks.

3.1 Dataset

The experiments operate on REMBRANDT dataset, a collection of Molecular Brain Neoplasia Data available from the Cancer Imaging Archive (TCIA), a freely accessible data repository [24]. This dataset was collaboratively developed by Thomas Henry Ford Hospitals (Detroit, MI, USA) and Jefferson University (Philadelphia, PA, USA). TCIA-REMBRANDT data comprises magnetic resonance imaging (MRI) scans along with clinical information, presenting a diverse range of tumor types and multiple MRI sequences, such as FLAIR (Fluid-Attenuated Inversion Recovery), T2-weighted, T1-weighted, and T1 post-contrast images. The dataset comprises MRI data from 130 patients, classified into four distinct brain tumor categories: Ependymoma (EPI), Oligodendroglioma (OLI), Astrocytoma (AST), and Glioblastoma-multiforme (GBM). The distribution of samples across each tumor type is as follows: GBM: 539 samples; OLI: 349 samples; AST: 557 samples; EPI: 431 samples; and normal: 1041 samples [25]. Figure 2 displays sample images from the REMBRANDT dataset.

3.2 Data Pre-processing and data augmentation

Improving data quality for classification tasks begins with a crucial initial step: data pre-processing. This step holds a key role in enhancing the overall performance of the model. Within the dataset, all MRI sequences undergo resizing and intensity normalization. This is imperative due to variations in image intensity across different MRI scans, arising from distinct imaging protocols and parameters. Each MRI sequence captures certain tumor characteristics. Relying solely on the classification with a single MRI sequence may yield suboptimal performance. Recognizing that each MRI sequence contributes essential features, a comprehensive approach considers all sequences. By amalgamating information from multiple sequences, crucial features are extracted, leading to an improvement in model performance. Consequently, post pre-processing, the images are merged to form multimodal data. This integration enhances the dataset's richness and aids in achieving more robust and accurate classification outcomes. The algorithm to generate multimodal data from MRI sequences is given below

Data augmentation

Deep learning procedures necessitate gigantic amount of data to design the model and to avoid over fitting. Limited available data is the drawback in health care. To overcome this drawback and to create

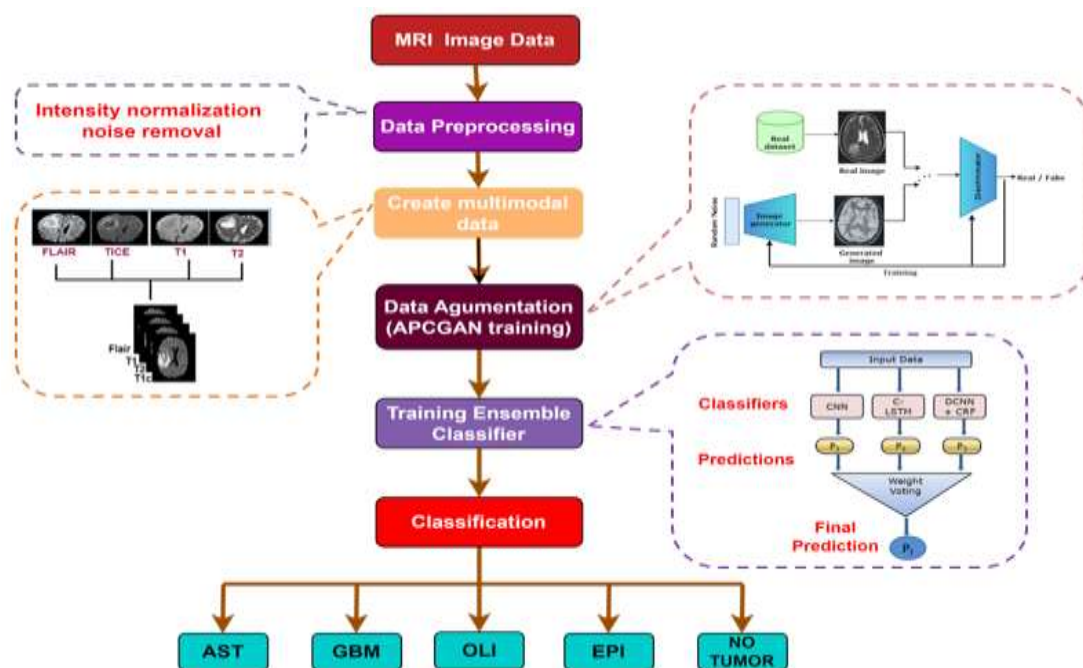


Figure 1. The global picture of proposed brain tumor classification process. AST: Astrocytoma, GBM: Glioblastoma multiforme, OLI: Oligodendroglioma, EPI: Ependymoma

Sample Images from Each Class

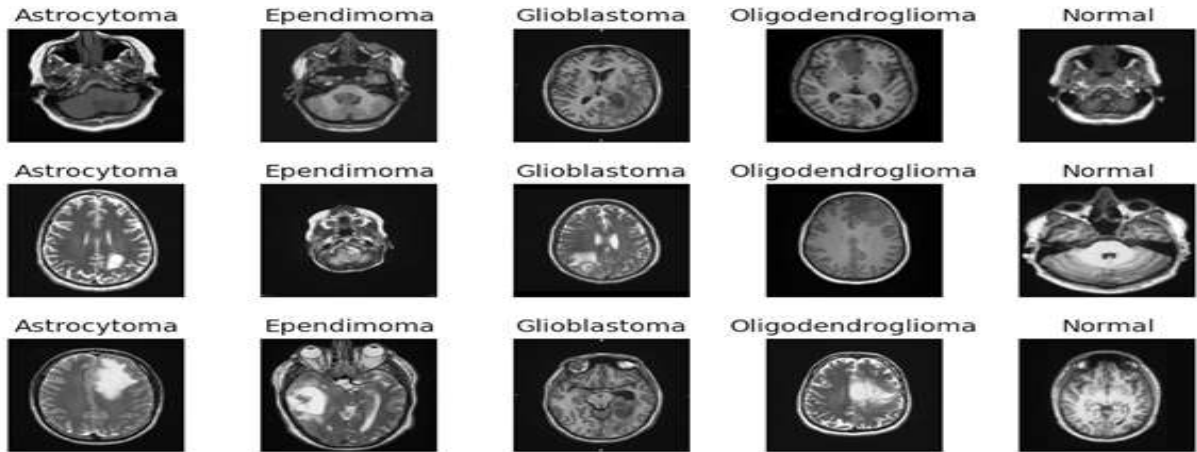


Figure 2. Sample images from REMBRANDT dataset

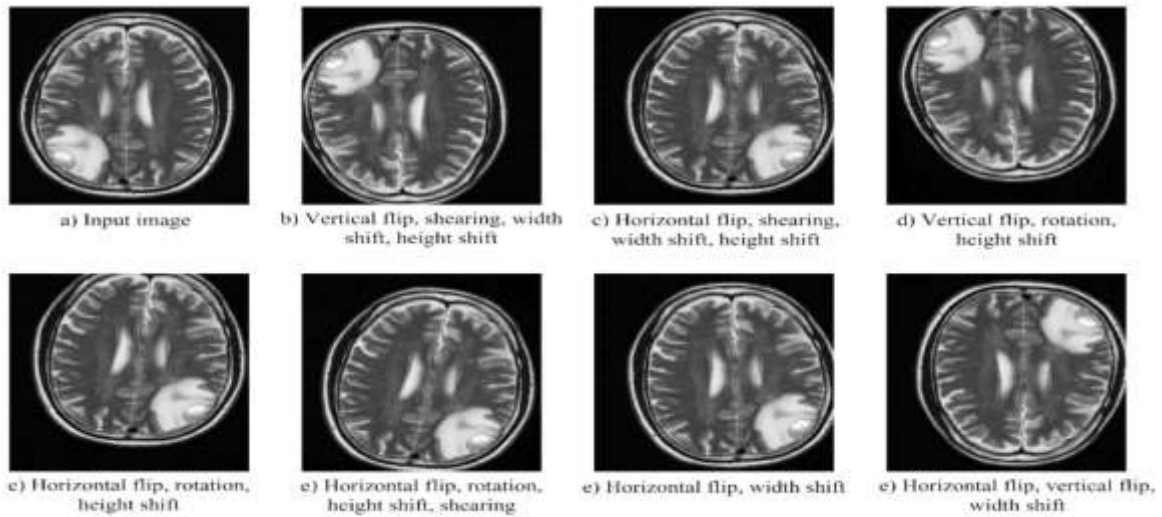


Figure 3. Sample images from dataset 1

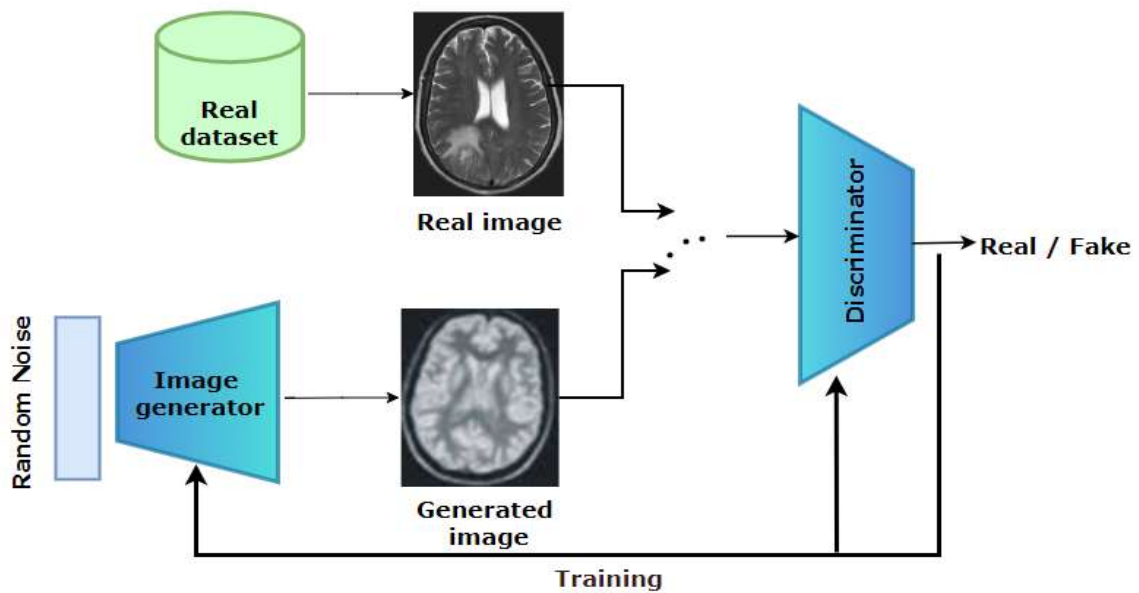


Figure 4. Adaptive Progressive Convolutional Generative Adversarial Networks

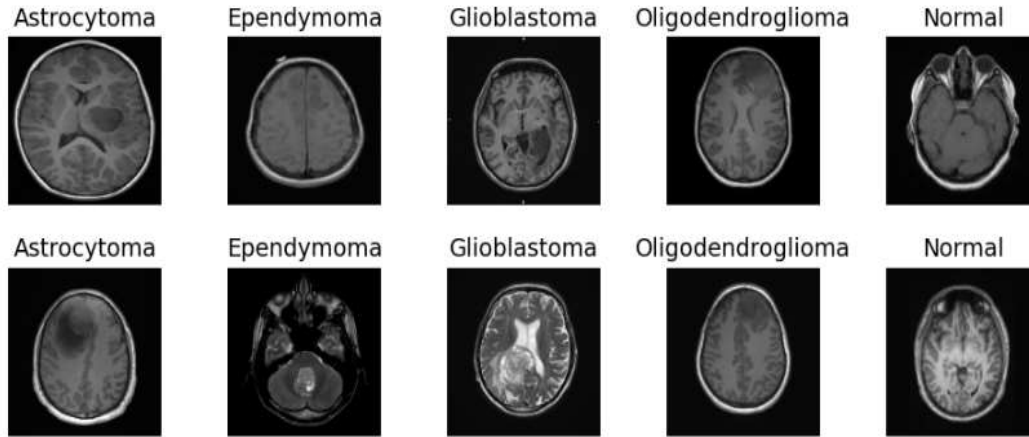


Figure 5: Sample images generated using APCGAN

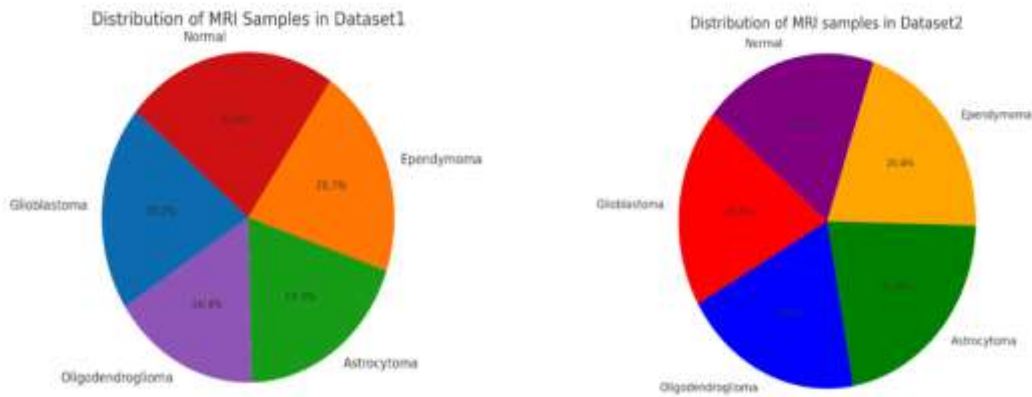


Figure 6. Pie charts showing the sample distribution in dataset1 and dataset2

Algorithm 1: Incorporating multimodal data

Input: MRI sequences (T1-weighted, contrast-enhanced T1-weighted, T2-weighted, and FLAIR) of same patient.

- Step 1: Preprocess the MRI images to ensure they are in the same orientation and voxel size.
- Step 2: Apply intensity normalization to each MRI modality.
- Step 3: Use a registration algorithm to align (same orientation and voxel size) the MRI modalities.
- Step 4: Concatenate the registered MRI modalities into a 4D tensor.

Output: A 4D tensor containing all four MRI modalities for a single patient.

A Registration algorithm is used to align the orientation and voxel size of the images.

Algorithm 2: Registration algorithm

Input: Load MRI Modalities A and B. Let the modalities be represented $A(x,y,z)$ and $B(x,y,z)$, where $x,y,$ and z denote the spatial coordinates in the image volume.

Step1: Check and Correct the Orientation of the Images

- a. If both images are in the neurological orientation, proceed.

- b. If not, perform orientation correction:
 - a. Determine the rotation angles Θ for A and B to align them to the neurological orientation. Compute the orientation difference $\Delta\Theta$ with respect to a standard orientation.
 - b. Apply the rotation or transformation to both images:

$$A'(x',y',z')=R(\Theta A)\cdot A(x,y,z)$$

$$B'(x',y',z')=R(\Theta B)\cdot B(x,y,z)$$

Where A' and B' are the reoriented images, and R(Θ) is the rotation or affine transformation matrix applied to each point (x,y,z) in the images.

Step2: Normalize the Voxel Size

- a. Check if the voxel sizes of both images A and B are the same.
- b. If the voxel sizes are the same, skip this step.
- c. If not, perform voxel size normalization:
 - i. Calculate the voxel size (d_x, d_y, d_z) for each image.
 - ii. Identify the image with the larger voxel size, say d_{xA}, d_{yA}, d_{zA} for A and d_{xB}, d_{yB}, d_{zB} for B.
 - iii. Resample the image with the larger voxel size to match the voxel size of the other image:

$$A''(x'',y'',z'')=\text{Interpolate}(A'(x',y',z'),d_{x\text{target}},d_{y\text{target}},d_{z\text{target}})$$

$$B''(x'',y'',z'')=\text{Interpolate}(B'(x',y',z'),d_{x\text{target}},d_{y\text{target}},d_{z\text{target}})$$

Where A'' and B'' are the images with normalized voxel sizes, and

$d_{x\text{target}}, d_{y\text{target}}, d_{z\text{target}}$ are the target voxel dimensions, chosen based on the smaller voxel sizes between A' and B'. The nearest neighbor interpolation function is applied.

Output: The MRI modalities A and B are now in the same orientation and voxel size, allowing for proper integration of multimodal data.

new training examples we apply data augmentation. Data augmentation applies random and controlled transformations to available images to create new training samples. This technique is useful to theatrically surge the size and diversity of the dataset using different transformations [26]. For the optimal training and validation of our model, we established two datasets named dataset1 and dataset2. The RAMBRANDT dataset forms the core of both datasets. In the creation of dataset1, we applied classical augmentation methods, including width shifting, height shifting, shear intensity, horizontal flip, and vertical flip. Post-augmentation, the sample distribution in dataset1 is as follows: GBM: 1417 samples; OLI: 1147 samples; AST: 1354 samples; EPI: 1455 samples; and normal: 1641 samples. The sample images from dataset1 are shown in figure3.

The generation of dataset2 is facilitated through the implementation of Adaptive Progressive Convolutional Generative Adversarial Networks (APCGAN). In 2014, Goodfellow and colleagues introduced a framework for generative adversarial networks (GANs). These networks aim to produce authentic images capable of deceiving a discriminator network, which distinguishes between original and replicated images [27]. The proposed approach leverages APCGAN shown in figure 4, a

specialized GAN architecture, to synthesize high-resolution images. Specifically tailored for generating realistic tumor images, APCGAN exhibits progressive growth and adaptability throughout the training and generative processes. The model commences with a modestly scaled generator and discriminator, gradually augmenting their complexity as the training advances [28]. Figure 5 displays the sample images generated by APCGAN from dataset2, while Figure 6 presents a pie chart illustrating the distribution of samples between dataset1 and dataset2.

APCGAN embraces progressive growing mechanism where it starts spawning low-resolution images and progressively increases the quality of images in the course of training. It also incorporates adaptive mechanism to adjust the network architecture and handles variations in image complexity [29]. When the discriminatory network is in the active state, it reduces the cross-entropy to the smallest possible value. The cost function is defined as follows in terms of mathematics:

$$H(x_i, y_i) = -y \log D(x_i) - (1 - y_i) \log(1 - D(x_i)) \quad (1)$$

The loss is computed as follows for an "n" number of iterations:

$$H(x_i, y_i) = \sum_{i=1}^N y_i \log D(x_i) - \sum_{i=1}^N (1 - y_i) \log(1 - D(x_i)) \tag{2}$$

Various multi-stage generative techniques have been proposed. For instance, the Composite GAN uses numerous generators to spawn distinct portions of an image. On the other hand, the ensemble methods use numerous training procedures to produce realistic images [30]. Researchers have started using GANs in medical imaging to perform image-to-image translation, which includes segmentation, cross modality translation, and super-resolution imaging. A recent study conducted by a team of researchers revealed that they can perform whole-MR image augmentation using a GAN [31]

3.3 Ensemble of CNN, C-LSTM and DCNN+CRF with weighted voting

Ensemble learning is a deep learning methodology, which associates multiple individual models, referred to as base learners or base classifiers, in order to obtain more accurate and robust results compared to any individual model. The underlying concept of this learning approach is to leverage the prophecies of various models, such that the powers of certain models can reimburse for the flaws of others, ultimately resulting in enhanced overall performance. Algorithm 3 gives the detailed working of ensemble model with weighted voting

approach. The ensemble classifiers, similar to single classifiers, are robust classifiers due to the utilization of weights to assess the accuracy of an individual classifier on a specific or complete subset of the dataset [32].

The weighted voting approach integrates the outputs of multiple classifiers using a weighted voting scheme. The weights assigned to every classifier can be determined centred on individual performance. The operation of the anticipated ensemble method with weighted voting is depicted in figure 7.

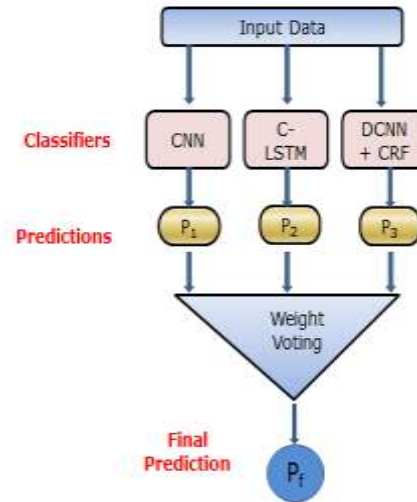


Figure 7. Ensemble of CNN, C-LSTM and DCNN+CRF with weighted voting strategy

Input: Multi modal data Deep Convolutional Neural Network

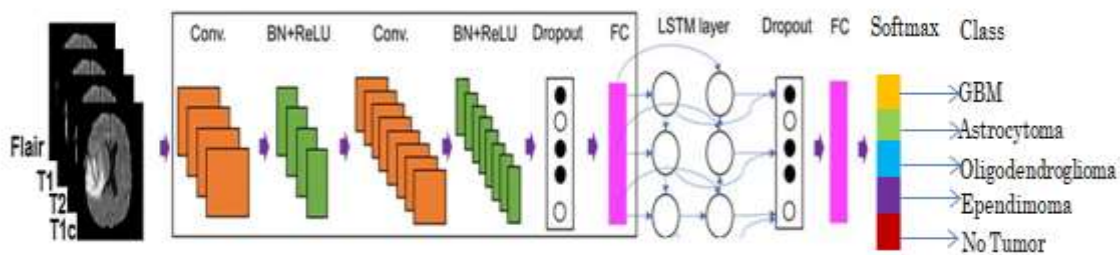


Figure 8. The architecture of deep C-LSTM method for multi class classification

Table 1. Performance analysis of different algorithms on dataset1

Algorithm	Dataset	Accuracy	Precision	Recall	F1-Score
Convolutional Neural Network (CNN)	Dataset1	0.824	0.791	0.850	0.811
Convolutional Long-Short-Term Memory (C-LSTM)	Dataset1	0.851	0.823	0.851	0.861
Deep Convolutional Neural Network + Conditional Random Fields (DCNN+CRF)	Dataset1	0.894	0.857	0.890	0.891
Ensemble of CNN, C-LSTM and DCNN + CRF with weighted voting	Dataset1	0.939	0.917	0.934	0.918

Table 2. Performance analysis of different algorithms on dataset2

Algorithm	Dataset	Accuracy	Precision	Recall	F1-Score
Convolutional Neural Network (CNN)	Dataset2	0.921	0.890	0.941	0.927
Convolutional Long-Short-Term Memory (C-LSTM)	Dataset2	0.944	0.926	0.960	0.948
Deep Convolutional Neural Network + Conditional Random Fields (DCNN+CRF)	Dataset2	0.961	0.945	0.976	0.960
Ensemble of CNN, C-LSTM and DCNN + CRF with weighted voting	Dataset2	0.994	0.991	0.980	0.992

Table 3. Performance comparison of proposed model with different methods used in literature

Author	Method	Accuracy
Zahoor et al. (2022)	Hybrid Boosted and Ensemble Learning	99.13
S. Montaha et al. (2022)	TimeDistributed-CNN-LSTM Hybrid Approach	98.90
Alsubai et al. (2022)	Ensemble Deep Learning	99.10
Alsubai et al. (2022)	Ensemble Deep Learning	97.12
Murthy et al. (2022)	Ensemble with Adaptive Fuzzy Deformable Fusion	98.26
Zobeda Hatif Naji Al-azzwi et al. (2023)	Cluster Ensemble and Deep Super Learner	96.60
Suraj Patil et al (2023)	Hybrid Optimized Multi-features Analysis	97.77
K. V. Archana et al. (2023)	Deep Features and Machine Learning Classifiers Ensemble	97.7
Proposed method	Ensemble of CNN, C-LSTM and DCNN+CRF with weighted voting	99.40

Algorithm 3: Ensemble learning with weighted voting approach

Input: A set of base models (CNN, C-LSTM, DCNN + CRF) with associated predictions. Weights for each base model, representing their relative importance.

Steps:

- 1) Initialize the ensemble with a list of base models and their corresponding weights. If no weights are provided, assume uniform weights (equal importance for all models).
- 2) Train each base model on the training data. This step may involve fitting the models to the features and labels in a supervised learning task.
- 3) For a new input or test data point: a. Use each base model to make a prediction. b. Multiply each prediction by its corresponding weight. c. Sum the weighted predictions for each model.
- 4) Select the class or value with the highest sum as the final prediction for classification or regression tasks, respectively.

Output: A final prediction based on weighted voting.

Convolutional Neural Networks (CNN)

In computer vision applications, Convolutional Neural Networks (CNNs) primarily accomplish image classification, object detection, and image recognition tasks. The CNN leverages its ability to simulate the behaviour of neurons in the human

brain to learn hierarchical representations of visual data. Numerous researchers have achieved significant advancements in their respective fields by employing CNN techniques. Within the CNN architecture, the convolutional layer plays a decisive part. In this layer, a convolution operation is applied

using a kernel, resulting in the generation of a feature map. This convolution operation can be accurately expressed by equation 3, where the variable "I" symbolizes the input and "K" signifies the kernel [33].

$$S(i, j) = \sum_m \sum_n I(m, n) * K(i - m, j - n) \quad (3)$$

The value within a feature chart is linked to the preceding layer via kernel weights. By stacking multiple convolutional layers, we can extract increasingly abstract features. As we progress deeper into the system, the initial steps extract higher-level features, while subsequently learning more low-level features. Following the convolution operation, an activation operation is put in to each portion of the feature map to instigate non-linearity [34]. In this study, we employ the Rectified Linear Unit (ReLU) activation function represented in equation (4).

$$f(x) = \max(0, x) \quad (4)$$

Pooling technique entails the placement of a two-dimensional filter over a channel in a map, followed by the identification of the characteristics that are encompassed within its coverage region. Layering techniques are employed to shrink the overall dimensions of the map. The computation of the output resulting from pooling can be achieved through the utilisation of a feature map characterised by the dimensions of nc, nw, and h. The architecture of Convolutional Neural Networks (CNNs) incorporates hidden layers that enable the reduction of image size while preserving the fundamental attributes of the original image. The convolutional neural network (CNN) employs diverse pooling methods to effectively decrease the dimensionality of the input image while preserving its information content [35]. Finally in the fully connected layer we used softmax activation to present output in multiple classes. The softmax activation is represented as in equation 5. Here the input vector is "y" and "n" is the number of classes.

$$s(y)_i = \frac{e^{y_i}}{\sum_{j=1}^n e^{y_j}} \quad (5)$$

Deep Convolutional LSTM

Convolutional neural networks (CNNs) united with long short-term memory (LSTM) has demonstrated promising results on an assortment of complex computer vision applications. Both CNN and LSTM methods are known for their power and robustness against noise. However, they can be computationally expensive when used individually. To answer this issue, we recommend the practice of a deep convolutional-LSTM (C-LSTM) approach for classifying brain tumors. The structural design of deep C-LSTM methodology is illustrated in figure 4. The deep CNN component is designed to extract

relevant and useful features, while the LSTM component is employed for tumor classification into five distinct classes as well as to enhance the accuracy of classification [5].

The deep CNN architecture is made up of two identical convolutional components, with dissimilar factors. These modules include a convolutional layer, the rectified linear unit (ReLU) activation function with batch normalization (BN). The convolutional layers employ same filter. On the other hand, LSTM systems are a variant of recurrent neural networks that excel in identifying order dependencies in sequence expectation problems. Batch normalization is used to normalize the data between CNN layers, while ReLU introduces non-linearity to overcome the issue of vanishing gradients [34]. To prevent over-fitting during training of the C-LSTM network, two dropout layers are introduced. These dropout layers improve generalization error and reduce the required training time as shown in figure 8. Finally, softmax activation function is employed to convert the output from fully connected layer into logic numbers representing probabilities [36].

network, wherein it undergoes changes over time. This memory cell comprises three dissimilar gates: the input, forget and output gates. The forget gate receives input in the form of output value from the previous instance and input value from current instance. The forget gate's output (ft) is determined by the equation (6), with ft's value confined within the range of 0 to 1. The forget gate's parameters encompass the weight (Wf), bias (bf), the preceding instance output (ht-1) and present input (xt), and [36].

The input gate receives output of last instance and the present as input. The gate outcome is calculated using equation (7), where the parameters weight (Wi), bias (bi), present input (xt), and the yield of the earlier instance (ht-1) are used. Cell state is computed using equation (8) with the parameters weight (Wc) of the input gate and bias (bc). The output gate outcome is computed using parameters weight (Wo) and bias (bo) by equation (9). The LSTM output is obtained by multiplying the outcome of output gate and cell state using equation (10). The sigmoid activation function is utilized in all the gates, while the final layer uses the tanh activation function [37].

$$ft = \sigma(Wf \cdot [ht - 1, xt] + bf) \quad (6)$$

$$it = \sigma(Wi \cdot [ht - 1, xt] + bi) \quad (7)$$

$$ct = \tanh(Wc \cdot [ht - 1, xt] + bc) \quad (8)$$

$$ot = \sigma(Wo \cdot [ht - 1, xt] + bo) \quad (9)$$

$$ht = ot * \tanh(ct) \quad (10)$$

DCNN+CRF

We combine Conditional Random Fields (CRF) with Deep Convolutional Neural Network (DCNN) to increase the accuracy of classification tasks [38,39]. Usually, CRF is used after DCNN to refine the DCNN's output by adding more information about the context and how things are arranged in space. The combination of DCNN and CRF is represented by the below equation:

$$P\left(\frac{y}{x}\right) = CRF(DCNN(X)) \quad (11)$$

In this equation, P(y|x) represents how likely the output labels (y) are based on the input image (x). DCNN(x) signifies the result of DCNN on the input image x [40]. CRF () represents using Conditional Random Fields on the output of the DCNN. The CRF part takes the DCNN's output, which could be pixel-wise probability maps or feature maps, and improves it by considering how adjacent pixels are arranged.

The CRF component examines the connections between nearby pixels, determining how they fit together, ensuring consistency of labels, and producing a smooth end result for segmentation or classification [41].

CRF is optimized based on the input image and DCNN output by maximizing their conditional probabilities. This optimization procedure modifies label assignments to improve consistency and accuracy [42]. The model benefits from the DCNN's robust feature mining abilities as well as the CRF's ability to modify the output by taking into account spatial dependencies by merging DCNN and CRF.

This combination improves the accuracy and coherence of segmentation or categorization findings, particularly in applications requiring the capture of specific information and spatial relationships within the image.

Weighted voting strategy

Usually, an ensemble classifier follows a two-step process: Selection and Combination. In our proposed method, we have selected three classifiers, namely CNN, C-LSTM, and DCNN+CRF. The amalgamation of these distinct classifiers' prophecies is achieved through various practices using diverse approaches. To accomplish this, we first select a set C = (C1, C2, ..., CN) with N classifiers by executing selected procedures to a particular dataset. Using a weighted voting approach, their individual predictions are combined. This strategy is commonly employed to combine predictions when the classifiers are not considered in

the same way. The classification accuracy of each classifier is determined by its coefficient (weight) as a result of evaluating it on the evaluation set D [43]. For the assessment of every constituent classifier, let's study a dataset D with M classes. The performance evaluation of every classifier Ci, where i = 1, 2, ..., N, is conducted using D. A N×M matrix W is then estimated as follows:

$$\begin{pmatrix} w_{1,1} & w_{1,2} & \dots & w_{1,M} \\ w_{2,1} & w_{2,2} & \dots & w_{2,M} \\ w_{N,1} & w_{N,2} & \dots & w_{N,M} \end{pmatrix}$$

Here each element Wi,j is calculated by

$$W_{i,j} = \frac{2p_j^{(c_j)}}{|D_j| + p_j^{(c_j)} + q_j^{(c_j)}} \quad (13)$$

The set Dj represents the illustrations of the dataset that belong to class j. The variables p_j^(c_j) and q_j^(c_j) indicate the count of accurate and erroneous predictions, respectively, anticipated by classifier Ci on Dj. The Wi,j (weight) corresponds to classifier Ci [44].

To determine the class y^ of an unfamiliar case x in the test dataset, equation (14) is employed.

$$\hat{y} = \arg \max_j \sum_{i=1}^N w_{i,j} \chi_A(C_i(x) = j) \quad (14)$$

This equation calculates the sum of the weights w(i,j) for each classifier Ci, multiplied by the characteristic function χ_A(C_i(x)=j), where χ_A is a vector that assigns a value of one to the j coordinate and zero to the remaining coordinates, centred on the forecast j∈A made by Ci classifier on instance x. The argmax function then yields the index value corresponding to the highest element in the resulting array. The set A represents the unique class labels, and M represents the number of elements in A. Building on the proposed methodology, this section discusses the empirical evaluation to demonstrate its effectiveness.

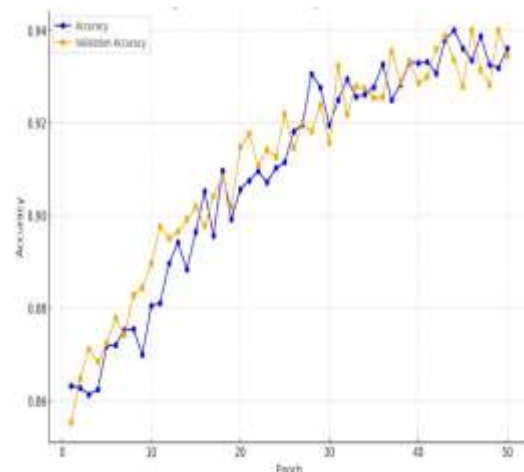


Figure 9. Progression of Model Accuracy on Dataset1

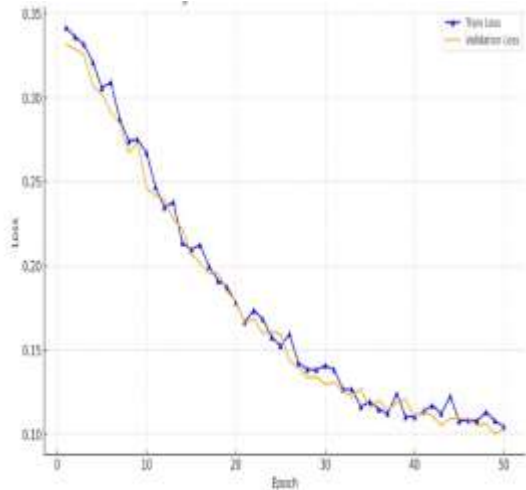


Figure 10. Ensemble Model Loss Minimization on Dataset1

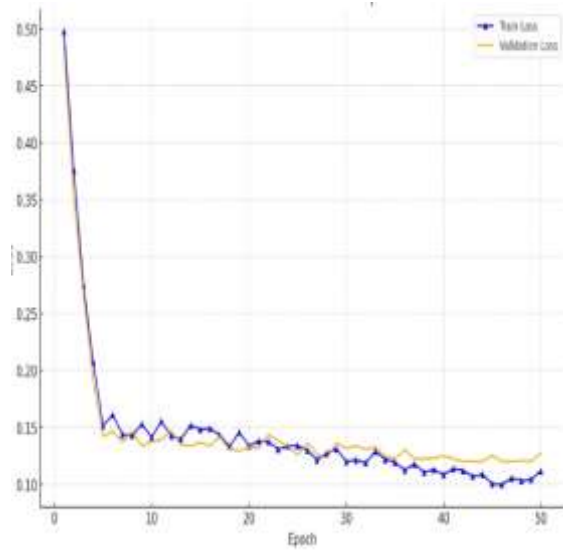


Figure 12. Training and Validation Loss of Ensemble Model on Dataset2

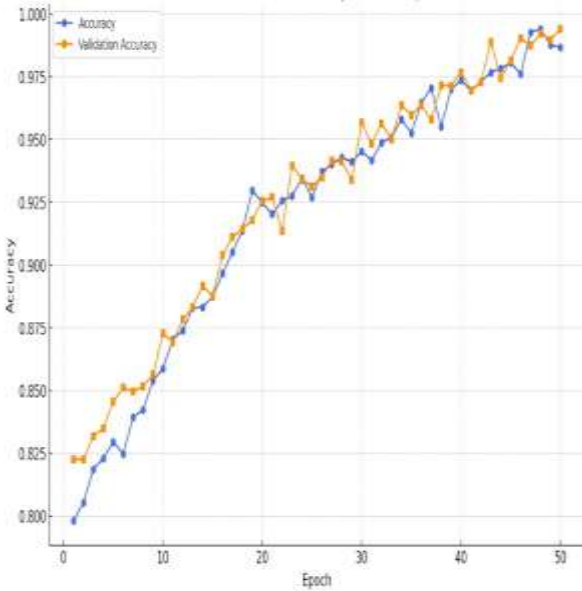


Figure 11. Training and Validation Accuracy of Ensemble Model on Dataset2

4. Experiments and Results:

In the proposed work, the entire dataset is partitioned into three distinct groups, namely a validation set (15%), a test set (15%) and training set (70%). The utilization of the training set is solely restricted to Ensemble method training process. The annotations utilized in the analysis are predicated upon 3D scans, which may exhibit imprecision and unwieldiness when applied to 2D slices. Furthermore, we eliminate images that do not meet the appropriate size requirements and those that lack proper labeling. To enhance their efficacy, the training images undergo zero-padding. The classification performance is assessed using the most prevalent and valuable parameters for image segmentation, namely F1-score, accuracy, recall, and precision measurements. The dataset names used in the comparison tables and graphs (Dataset 1, Dataset 2) were place holders to represent different datasets utilized for brain tumor classification. The graph in figure 9 delineates the evolution of accuracy for the proposed ensemble model trained on Dataset1 over a span of 50 epochs. The accuracy, signifying the proportion of correctly predicted instances, exhibits a steady ascent from the commencement of training, culminating at a peak value of 0.939. Notably, the model's performance on unseen validation data closely tracks the training accuracy, indicating effective generalization without significant overfitting. The convergence of training and validation accuracy towards the latter epochs implies the model's training progression is nearing optimization, with little expected gain from further training. The graph in figure 10 presents the trajectory of loss for the ensemble model on Dataset1. Loss, a quantifier of the model's error rate,

witnesses a significant reduction in the early training phase, reflecting the model's rapid initial learning and adjustment to the dataset's patterns. Afterward, the loss gradually decreases, showing the model getting better bit by bit. When the loss plateaus towards the end of the graph, it means the model has reached a point with very little error, and doing more training won't make a big difference. This shows that the ensemble model can effectively predict outcomes on Dataset1, marking a successful training effort.

The proposed ensemble model performance on Dataset2 over 50 training epochs is shown in figure 11.

At the beginning, the accuracy on both the training and validation sets goes up steadily, showing that the model is learning and making accurate predictions. As the epochs go on, the accuracy increase slows down, which is normal for complex models where they make big improvements at first and then smaller ones. The model shows strong performance by reaching validation accuracy close to 0.994, highlighting its ability to correctly classify the dataset. This behavior shows that the model can be reliable and used effectively in real-world applications.

Figure 12 displays the training and validation loss of a combined ensemble model, incorporating CNN, CLSTM, and DCNN + CRF, trained on Dataset2. The steep drop in the early epochs shows fast learning, indicating that the model rapidly reduces the loss as it learns to generalize from the data. As training progresses beyond the initial epochs, we observe the loss reduction stabilizing, reflecting the diminishing returns of further training as the model begins to converge to its optimal state. The training loss consistently remains slightly below the validation loss, suggesting the model is learning effectively without overfitting. The near convergence of both curves towards the end indicates a well-fitted model that has generalized well to the validation set, with minimal expected improvement in subsequent epochs.

According to the findings, it can be discerned that the ensemble method exhibits superior performance when compared to other algorithms such as CNN, C-LSTM, and DCNN+CRF. This superiority is evident by means of F1-score, precision, recall, and accuracy across all the datasets. Ensemble method shows higher performance in accurately segmenting and classifying tumors, achieving higher scores in evaluation parameters.

However, it is essential to acknowledge that the actual outcomes may differ based on the specific implementation, training parameters, and the datasets utilized for evaluation. The aforementioned results serve as a comparison of the algorithms'

efficacy on both datasets. It is worth noting that these results are merely illustrative and the actual performance may oscillate subject to specific application, training parameters, and dataset characteristics. The algorithms, namely CNN, C-LSTM, DCNN+CRF, and the ensemble method, have been scrutinized for their performance in brain tumor segmentation and classification consuming REMBRANDT datasets. A comprehensive depiction of various performance measures are found in Table1 and Table2

5. Discussion

Deep learning algorithms are very powerful that typically work well when trained on a gigantic amount of data. A major hurdle in analysing medical image is the obtainability of limited labelled training data. To overcome this, generally data augmentation and transfer learning strategies are commonly used. The APCGANs used in the proposed model provides best data augmentation for a given dataset. In this work we analysed the classification efficiency of multiple CNN grounded practices on two datasets. Among the analysed algorithms, ensemble method with weighted voting consistently outperforms CNN, C-LSTM, and DCNN+CRF, showcasing its effectiveness in brain tumor classification. The comparison across datasets highlights the impact of dataset characteristics on algorithm performance. From tables 1 and 2 we can observe that data augmentation plays an important role in achieving high accuracy. The APCGAN created realistic images compared to traditional augmentation procedures like rotation, flipping etc. we obtained high accuracy with ensemble method applied on dataset2. Performance measures such as accuracy, precision, recall and F1-score are used to measure the effectiveness and the figures 9 and 10 represents the comparisons of the metrics among the datasets

Accuracy: Accuracy is a measure that reflects the extent to which an algorithm's predictions align with the actual outcomes. It quantifies the ratio of accurately categorized instances to the total available samples. This measure is commonly employed to evaluate the correctness of varied methods. Among the algorithms, ensemble method achieved the highest accuracy on all datasets, ranging from 0.939 to 0.994. The lowest accuracy scores were obtained by CNN on the dataset1 (0.824), while C-LSTM (0.851) and DCNN+CRF (0.894). On dataset2 CNN scored an accuracy of (0.921), while C-LSTM (0.944) and DCNN+CRF (0.961). **Precision:** Based on the total expected positive instances, precision measures the fraction of appropriately identified correct samples. Ensemble method consistently showed the highest precision

values across all datasets, ranging from 0.917 to 0.991. On dataset1 CNN had the lowest precision (0.791), while C-LSTM (0.823) and DCNN+CRF (0.857). On dataset2 CNN scored precision (0.890), while C-LSTM (0.926) and DCNN+CRF (0.945). Recall: Based on the actual number of positive samples, recall is calculated as the percentage of positively identified samples out of the over-all positive samples. CNN achieved the lowest recall on the dataset1 (0.850). F1-Score: The F1-Score offers a well-rounded valuation of a model's performance by computing the harmonic mean of precision and recall. Ensemble method consistently achieved the highest F1-Score values across all datasets, ranging from 0.918 to 0.992. CNN had the lowest F1-Score on dataset1 (0.811). Figure 13 is performance comparison of different methods on dataset-1 and figure 14 is the performance comparison of different methods on dataset-2.

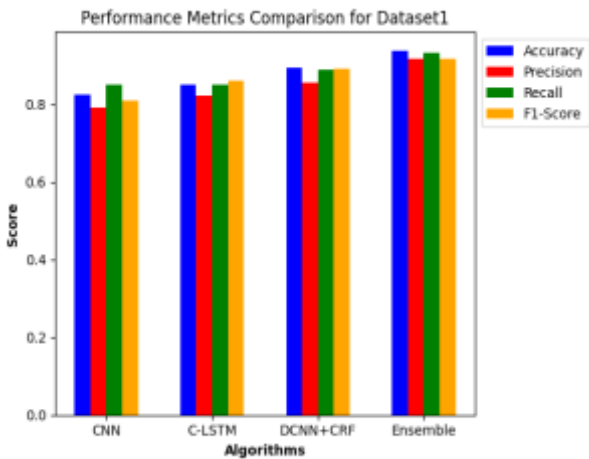


Figure 13. Performance comparison of different methods on dataset-1

On the datasets provided, the ensemble model outperformed CNN, C-LSTM, and DCNN+CRF models in terms of precision, recall, accuracy, and F1-Score. It achieved the best scores in every performance metric, proving its effectiveness in brain tumor segmentation and classification jobs. The proposed method accomplished an accuracy of 99.4% that highlights the superiority of ensemble model in classifying brain tumors. This accuracy of ensemble method was compared with various methods found in the literature, as available in Table 3.

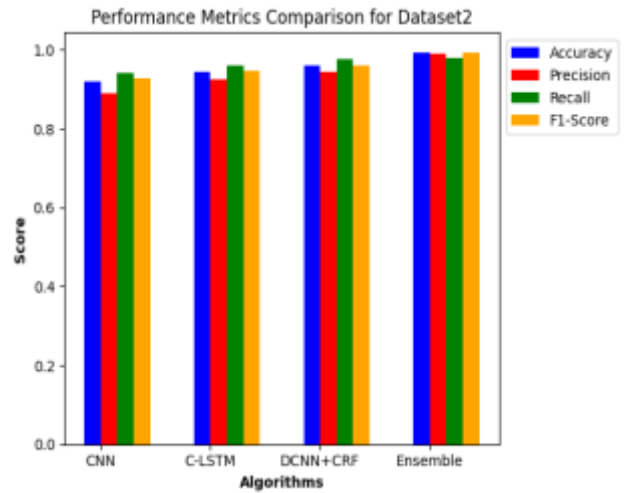


Figure 14. Performance comparison of different methods on dataset-2.

6. Conclusions

Deep learning techniques have made significant advancements in the arena of brain tumor classification. The fusion of convolutional neural networks (CNNs), ensemble learning, transfer learning, and deep supervision techniques has greatly improved the accuracy of tumor segmentation and classification. Our proposed model has presented promising results in accurately classifying various types of brain tumors, including Astrocytoma, Glioblastoma multiforme, oligodendroglioma, and Ependymoma, using MRI images. These advancements in model architectures and techniques have contributed to continuous improvements in tumor classification. Our proposed ensemble method utilizes three base classifiers, namely CNN, C-LSTM, and DCNN+CRF. To effectively train the model, we utilized the Adaptive Progressive Convolutional GANs (APCGANs) method for data augmentation. Overall, our ensemble method with a weighted voting strategy steadily outperforms the other algorithms (CNN, C-LSTM, and DCNN+CRF) across all datasets (Dataset1 and Dataset2). It achieves the highest performance measures among all algorithms, with an accuracy of 0.994 on dataset2. Additionally, the ensemble method achieves the highest precision, recall, and F1-score on dataset2, with measures of 0.991, 0.980, and 0.992, respectively. These results demonstrate the superior performance of ensemble methods, surpassing other tested algorithms. Brain tumor studied in the literature and reported [45-55].

Author Statements:

- **Ethical approval:** The conducted research is not related to either human or animal use.

- **Conflicts of Interest:** Regarding the publication of this paper, the authors affirm that they have no conflicts of interest.
- **Acknowledgement:** The authors declare that they have nobody or no-company to acknowledge.
- **Author contributions:** The authors declare that they have equal right on this paper.
- **Funding information:** The authors declare that there is no funding to be acknowledged.
- **Data Availability:** The report contains the data that were utilized in support of the results of this investigation. If more information is needed, it can be obtained from the corresponding author upon request.

References

- [1] Cancer statistics [Online]. Available: <https://www.cancer.net/cancer-types/brain-tumor/statistics>. Accessed: 17-Feb-2024
- [2] Jäkel Sarah, Dimou Leda, (2017). Glial Cells and Their Function in the Adult Brain: A Journey through the History of Their Ablation, *Frontiers in Cellular Neuroscience*, 11, doi: 10.3389/fncel.2017.00024
- [3] G.S. Tandel, M. Biswas, O.G. Kakde, A. Tiwari, H.S. Suri, M. Turk, B. K. Madhusudhan, L. Saba, J.S. Suri, (2019) A review on a deep learning perspective in brain cancer classification, *Cancers* 11(1);111, <https://doi.org/10.3390/cancers11010111>.
- [4] Rakesh Chandra Joshi, Rashmi Mishra, Puneet Gandhi, Vinay Kumar Pathak, Radim Burget, Malay Kishore Dutta, (2021). Ensemble based machine learning approach for prediction of glioma and multi-grade classification, *Computers in Biology and Medicine*, 137;104829, <https://doi.org/10.1016/j.compbiomed.2021.104829>
- [5] Parpura, V., Heneka, M.T., Montana, V., Oliek, S.H.R., Schousboe, A., Haydon, P.G., Stout, R.F., Jr, Spray, D.C., Reichenbach, A., Pannicke, T., Pekny, M., Pekna, M., Zorec, R. and Verkhratsky, A. (2012), Glial cells in (patho)physiology. *Journal of Neurochemistry*, 121: 4-27. <https://doi.org/10.1111/j.1471-4159.2012.07664.x>
- [6] Walker C, Baborie A, Crooks D, Wilkins S, Jenkinson MD. (2011). Biology, genetics and imaging of glial cell tumours. *Br J Radiol.* 2(2);S90-106. doi: 10.1259/bjr/23430927.
- [7] T.Deepa, Dr. Ch.D.V. Subba Rao, (2022). Deep Learning approaches for brain tumor segmentation and multiclass classification, *NeuroQuantology*, 20(16);1694-1706, DOI: 10.48047/NQ.2022.20.16.NQ880168
- [8] Zahoor, M.M.; Qureshi, S.A.; Bibi, S.; Khan, S.H.; Khan, A.; Ghafoor, U.; Bhutta, M.R. (2022). A New Deep Hybrid Boosted and Ensemble Learning-Based Brain Tumor Analysis Using MRI. *Sensors* 22;2726. <https://doi.org/10.3390/s22072726>
- [9] S. Montaha, S. Azam, A. K. M. R. H. Rafid, M. Z. Hasan, A. Karim and A. Islam, (2022). TimeDistributed-CNN-LSTM: A Hybrid Approach Combining CNN and LSTM to Classify Brain Tumor on 3D MRI Scans Performing Ablation Study, in *IEEE Access*, 10; 60039-60059, doi: 10.1109/ACCESS.2022.3179577.
- [10] Amin, J., Anjum, M. A., Sharif, M., Jabeen, S., Kadry, S., and Moreno Ger, P. (2022). A new model for brain tumor detection using ensemble transfer learning and quantum variational classifier. *Comput. Intell. Neurosci.* 3236305. doi: 10.1155/2022/3236305
- [11] Zahid Ullah, Muhammad Usman, Moongu Jeon, Jeonghwan Gwak, (2022) Cascade multiscale residual attention CNNs with adaptive ROI for automatic brain tumor segmentation, *Information Sciences*, 608;1541-1556, <https://doi.org/10.1016/j.ins.2022.07.044>.
- [12] S. Ahmad and P. K. Choudhury, (2022). On the Performance of Deep Transfer Learning Networks for Brain Tumor Detection Using MR Images, in *IEEE Access*, 10;59099-59114,
- [13] Alsubai S, Khan HU, Alqahtani A, Sha M, Abbas S and Mohammad UG (2022) Ensemble deep learning for brain tumor detection. *Front. Comput. Neurosci.* 16:1005617. doi: 10.3389/fncom.2022.1005617
- [14] Murthy, M.Y.B., Koteswararao, A. & Babu, M.S. (2022) Adaptive fuzzy deformable fusion and optimized CNN with ensemble classification for automated brain tumor diagnosis. *Biomed. Eng. Lett.* 12, 37–58. <https://doi.org/10.1007/s13534-021-00209-5>
- [15] Bhatele, K.R., Bhaduria, S.S. (2023). Multiclass classification of central nervous system brain tumor types based on proposed hybrid texture feature extraction methods and ensemble learning. *Multimed Tools Appl* 82, 3831–3858. <https://doi.org/10.1007/s11042-022-13439-1>
- [16] Syed Ali Nawaz, Dost Muhammad Khan & Salman Qadri (2022) Brain Tumor Classification Based on Hybrid Optimized Multi-features Analysis Using Magnetic Resonance Imaging Dataset, *Applied Artificial Intelligence*, 36:1, 2031824, DOI: 10.1080/08839514.2022.2031824
- [17] S. Asif, W. Yi, Q. U. Ain, J. Hou, T. Yi and J. Si, (2022). Improving Effectiveness of Different Deep Transfer Learning-Based Models for Detecting Brain Tumors From MR Images, in *IEEE Access*, 10;34716-34730, doi: 10.1109/ACCESS.2022.3153306.
- [18] Das, Suchismita, Bose, Srijib, Nayak, Gopal Krishna and Saxena, Sanjay. (2022) Deep learning-based ensemble model for brain tumor segmentation using multi-parametric MR scans *Open Computer Science*, 12(1);211-226. <https://doi.org/10.1515/comp-2022-0242>.
- [19] Kang, J.; Ullah, Z.; Gwak, J. (2021). MRI-Based Brain Tumor Classification Using Ensemble of Deep Features and Machine Learning Classifiers. *Sensors* 21;2222. <https://doi.org/10.3390/s21062222>

- [20] Garg, G., & Garg, R. (2021). Brain Tumor Detection and Classification based on Hybrid Ensemble Classifier. *ArXiv*, abs/2101.00216.
- [21] Ramya, P., Thanabal, M.S. & Dharmaraja, C. (2021) Brain tumor segmentation using cluster ensemble and deep super learner for classification of MRI. *J Ambient Intell Human Comput* 12;9939–9952. <https://doi.org/10.1007/s12652-021-03390-8>
- [22] Kimia Rezaei, Hamed Agahi & Azar Mahmoodzadeh (2020): A Weighted Voting Classifiers Ensemble for the Brain Tumors Classification in MR Images, *IETE Journal of Research*, DOI: 10.1080/03772063.2020.1780487.
- [23] Clark, K.; Vendt, B.; Smith, K.; Freymann, J.; Kirby, J.; Koppel, P.; Moore, S.; Phillips, S.; Maffitt, D.; Pringle, M.; et al. (2013). The Cancer Imaging Archive (TCIA): Maintaining and Operating a Public Information Repository. *J. Digit. Imaging* 26, 1045–1057.
- [24] Tandel, G.S.; Tiwari, A.; Kakde, O.G.; Gupta, N.; Saba, L.; Suri, J.S. (2023). Role of Ensemble Deep Learning for Brain Tumor Classification in Multiple Magnetic Resonance Imaging Sequence Data. *Diagnostics* 13, 481. <https://doi.org/10.3390/diagnostics13030481>
- [25] Gopal S. Tandel, Antonella Balestrieri, Tanay Jujaray, Narender N. Khanna, Luca Saba, Jasjit S. Suri, (2020) Multiclass magnetic resonance imaging brain tumor classification using artificial intelligence paradigm, *Computers in Biology and Medicine*, 122, 103804,
- [26] Meor Yahaya MS and Teo J (2023) Data augmentation using generative adversarial networks for images and biomarkers in medicine and neuroscience. *Front. Appl. Math. Stat.* 9:1162760. doi: 10.3389/fams.2023.1162760
- [27] Han, C. et al. (2020). Infinite Brain MR Images: PGGAN-Based Data Augmentation for Tumor Detection. In: Esposito, A., Faundez-Zanuy, M., Morabito, F., Pasero, E. (eds) *Neural Approaches to Dynamics of Signal Exchanges. Smart Innovation, Systems and Technologies*, vol 151. Springer, Singapore. https://doi.org/10.1007/978-981-13-8950-4_27
- [28] Jiamin Liang, Xin Yang, Yuhao Huang, Haoming Li, Shuangchi He, Xindi Hu, Zejian Chen, Wufeng Xue, Jun Cheng, Dong Ni, (2022). Sketch guided and progressive growing GAN for realistic and editable ultrasound image synthesis, *Medical Image Analysis*, 79, <https://doi.org/10.1016/j.media.2022.102461>.
- [29] Xue, Y., Xu, T., Zhang, H., Long, L.R., Huang, X. (2018). SegAN: Adversarial network with multi-scale L1 loss for Medical Image Segmentation. *Neuroinformatics*, 16(3): 383-392. <https://doi.org/10.1007/s12021-018-9377-x>
- [30] Nema, S., Dudhane, A., Murala, S., Naidu, S. (2020). RescueNet: An unpaired GAN for brain tumor segmentation. *Biomedical Signal Processing and Control*, 55: 101641. <https://doi.org/10.1016/j.bspc.2019.101641>
- [31] N. Remzan, K. Tahiry and A. Farchi, "Ensemble Transfer Learning for Brain Tumor Classification," 2022 5th International Conference on Advanced Communication Technologies and Networking (CommNet), Marrakech, Morocco, 2022, pp. 1-6, doi: 10.1109/CommNet56067.2022.9993831.
- [32] Deep Learning Ian Goodfellow, Yoshua Bengio, Aaron Courville - Deep Learning (2017, MIT).pdf
- [33] Pereira, S., Pinto, A., Alves, V., Silva, C.A. (2016). Brain tumor segmentation using convolutional neural networks in MRI images. *IEEE Transactions on Medical Imaging*, 35(5): 1240-1251. <https://doi.org/10.1109/TMI.2016.2538465>
- [34] M. Artzi et al., (2021). Classification of Pediatric Posterior Fossa Tumors Using Convolutional Neural Network and Tabular Data, *IEEE Access*, 9;91966-91973, doi: 10.1109/ACCESS.2021.3085771.
- [35] Y. Liu et al., (2020). Deep C-LSTM Neural Network for Epileptic Seizure and Tumor Detection Using High-Dimension EEG Signals, in *IEEE Access*, 8, doi: 10.1109/ACCESS.2020.2976156.
- [36] Sushovan Chaudhury, Kartik Sau, (2023). A BERT encoding with Recurrent Neural Network and Long-Short Term Memory for breast cancer image classification, *Decision Analytics Journal*, 6, <https://doi.org/10.1016/j.dajour.2023.100177>
- [37] S. Shanthi, S. Saradha, J.A. Smitha, N. Prasath, H. Anandakumar, (2022). An efficient automatic brain tumor classification using optimized hybrid deep neural network, *International Journal of Intelligent Networks*, 3, <https://doi.org/10.1016/j.ijin.2022.11.003>.
- [38] Kamnitsas, K., Ledig, C., Newcombe, V.F., Simpson, J.P., Kane, A.D., Menon, D.K., Glocker, B. (2017). Efficient multi-scale 3D CNN with fully connected CRF for accurate brain lesion segmentation. *Medical image analysis*, 36: 61-78. <https://doi.org/10.1016/j.media.2016.10.004>
- [39] Hussain, S., Anwar, S.M., Majid, M. (2018). Segmentation of glioma tumors in brain using deep convolutional neural network. *Neurocomputing*, 282: 248-261. <https://doi.org/10.1016/j.neucom.2017.12.032>
- [40] Zhao, X., Wu, Y., Song, G., Li, Z., Zhang, Y., Fan, Y. (2018). A deep learning model integrating FCNNs and CRFs for brain tumor segmentation. *Medical image analysis*, 43: 98-111. <https://doi.org/10.1016/j.media.2017.10.002>
- [41] Hu, K., Gan, Q., Zhang, Y., Deng, S., Xiao, F., Huang, W., Gao, X. (2019). Brain tumor segmentation using multi-cascaded convolutional neural networks and conditional random field. *IEEE Access*, 7: 92615-92629. <https://doi.org/10.1109/ACCESS.2019.2927433>
- [42] J. Dhar, (2021). Multistage Ensemble Learning Model With Weighted Voting and Genetic Algorithm Optimization Strategy for Detecting Chronic Obstructive Pulmonary Disease, in *IEEE Access*, 9;48640-48657, doi: 10.1109/ACCESS.2021.3067949.
- [43] Livieris, I.E.; Kanavos, A.; Tampakas, V.; Pintelas, P. (2019). A Weighted Voting Ensemble Self-Labeled Algorithm for the Detection of Lung Abnormalities from X-Rays. *Algorithms* 12, 64. <https://doi.org/10.3390/a12030064>

- [44] Alturki, N.; Umer, M.; Ishaq, A.; Abuzinadah, N.; Alnowaiser, K.; Mohamed, A.; Saidani, O.; Ashraf, I. (2023). Combining CNN Features with Voting Classifiers for Optimizing Performance of Brain Tumor Classification. *Cancers* 15, 1767. <https://doi.org/10.3390/cancers15061767>
- [45] MOHAMMED, H. A., Adem, Şevki, & SAHAB, K. S. (2023). Optimal Examination Ways to follow up patients effected by COVID-19: case study in Jalawla General Hospital in Iraq. *International Journal of Applied Sciences and Radiation Research* , 1(1). Retrieved from <https://ijasrar.com/index.php/ijasrar/article/view/5>
- [46] MOHAMMED, H. A., Adem, Şevki, & SAHAB, K. S. (2024). Estimation the Biochemical parameters Changes in Blood of Corona Virus Patients in Iraq in Order to Support the Timely Decision Needs . *International Journal of Applied Sciences and Radiation Research* , 1(1). Retrieved from <https://ijasrar.com/index.php/ijasrar/article/view/4>
- [47] OZSOY, S., & DELIBAS, E. A. O. (2023). The Effect of Fragment C of Tetanus Toxin on Memory Deficits in a Rat Model of Alzheimer’s Disease . *International Journal of Computational and Experimental Science and Engineering*, 9(3), 254–259. Retrieved from <https://ijcesen.com/index.php/ijcesen/article/view/264>
- [48] M, V., V, J., K, A., Kalakoti, G., & Nithila, E. (2024). Explainable AI for Transparent MRI Segmentation: Deep Learning and Visual Attribution in Clinical Decision Support. *International Journal of Computational and Experimental Science and Engineering*, 10(4);575-584. <https://doi.org/10.22399/ijcesen.479>
- [49] BACAK, A., ŞENEL, M., & GÜNAY, O. (2023). Convolutional Neural Network (CNN) Prediction on Meningioma, Glioma with Tensorflow. *International Journal of Computational and Experimental Science and Engineering*, 9(2), 197–204. Retrieved from <https://ijcesen.com/index.php/ijcesen/article/view/210>
- [50] N, S., S. Prabu, V, T. K., D, C., K, B., & B. Buvaneswari. (2024). Computer Aided Based Performance Analysis of Glioblastoma Tumor Detection Methods using UNET-CNN. *International Journal of Computational and Experimental Science and Engineering*, 10(4);753-762. <https://doi.org/10.22399/ijcesen.515>
- [51] Vijayadeep GUMMADI, & Naga Malleswara Rao NALLAMOTHU. (2025). Optimizing 3D Brain Tumor Detection with Hybrid Mean Clustering and Ensemble Classifiers. *International Journal of Computational and Experimental Science and Engineering*, 11(1)124-134. <https://doi.org/10.22399/ijcesen.719>
- [52] Prathipati Silpa Chaitanya, & Susanta Kumar Satpathy. (2024). Advancing Brain Tumour Detection and Classification: Knowledge Distilled ResNeXt Model for Multi-Class MRI Analysis. *International Journal of Computational and Experimental Science and Engineering*, 10(4);1610-1623. <https://doi.org/10.22399/ijcesen.730>
- [53] Özlen, M. S., Cuma, A. B., Yazıcı, S. D., Yeğın, N., Demir, Özge, Aksoy, H., ... Günay, O. (2024). Determination of Radiation Dose Level Exposed to Thyroid in C-Arm Scopy. *International Journal of Applied Sciences and Radiation Research* , 1(1). Retrieved from <https://ijasrar.com/index.php/ijasrar/article/view/13>
- [54] Abuş, F., Gürçalar , A., Günay, O., Tunçman , D., Kesmezacar, F. F., & Demir, M. (2024). Quantification of Lens Radiation Exposure in Scopy Imaging: A Dose Level Analysis. *International Journal of Applied Sciences and Radiation Research* , 1(1). Retrieved from <https://ijasrar.com/index.php/ijasrar/article/view/11>
- [55] SHARMA, M., & BENIWAL, S. (2024). Feature Extraction Using Hybrid Approach of VGG19 and GLCM For Optimized Brain Tumor Classification. *International Journal of Computational and Experimental Science and Engineering*, 10(4);1728-1734. <https://doi.org/10.22399/ijcesen.714>